ACOUSTIC EMISSION AND FATIGUE CHARACTERISTICS OF TYPICAL BRIDGE STEELS

Theodore Hopwood and J. H. Havens, Division of Research, Kentucky Department of Transportation

Acoustic emission monitoring was used during tensile tests of low-carbon structural steels to determine the physical characteristics of the acoustic emission phenomena. Results indicate that acoustic emissions are caused by micro-plastic deformation processes (i.e., dislocation motion).

A series of axial-fatigue tests was performed on several types of structural steels, some of which had extensive service in bridges. There was no apparent relation between specimen load histories and subsequent performance in fatigue tests. Tensile tests of specimens subjected to extensive fatigue testing, at stresses below the yield strength of the material, revealed no major difference in mechanical properties or acoustic emission response due to their fatigue histories.

Further tests revealed that acoustic emission testing in the frequency range of 100-300 kHz has the physical capability of detecting cracks on large structural steel members. This may prove beneficial for the comprehensive nondestructive evaluation of steel bridges.

Summary

Most bridges which have failed have succumbed to brittle failures. However, fatigue failure of bridges is a constant danger. Bridges are being subjected to heavier traffic loads and higher traffic volumes. The increased use of welding in bridge construction has also increased the hazard of fatigue failures.

The Division of Research, Kentucky Bureau of Highways, has been concerned with the problem of bridge fatigue. The Division of Research approached this problem from a statistical viewpoint, attempting to determine bridge fatigue lives from traffic loading patterns. However, a need existed to determine the mechanical behavior of bridge steels which had seen long service in fatigue environments. Acoustic emission, a new nondestructive evaluation tool, showed some potential for providing data about the loading history of a material. A study was initiated to investigate these subjects.

Acoustic emissions (AE) are transient elastic waves generated in a material subject to external stress. In metals, sensitive electronic 'listening' devices must be used detect acoustic emission. A Dunegan Model 3000 acoustic emission detector was used in this study.

A series of tensile and compressive tests was performed on mild steel and aluminum specimens to determine the physical sources of acoustic emission. Steel specimens in both the annealed and cold-rolled states produced acoustic activity which was best explained as being caused by elements of microplasticity (i.e., dislocation motion). The behavior of aluminum tensile and compressive specimens reinforced this view. AE activity was found to be irreversible with increased loading. If a specimen was partially loaded and relieved, no emission was detected until the specimen was stressed to a higher level. This behavior is termed the Kaiser effect.

Tensile specimens were prepared from an old eyebar from the C & O bridge at Covington. The eyebar had lain in a storage yard for a year since the bridge had been demolished. Tests revealed that strain aging had occurred, preventing AE monitoring from detecting the specimens' loading history.

A series of axial-fatigue tests was initiated using eyebar specimens and five specimens from a special batch of replica steel furnished by National Steel Corporation. Twelve specimens each came from two additional types of structural steels. These steels, probably ASTM A 7, came from rivited bridge members that had suffered fatigue failures.

The fatigue tests were performed by Metcut Research Associates of Cincinnati, Ohio, on a Baldwin-Lima-Hamilton, IV-20 fatigue machine. The eyebar and replica specimens were tested at various stress ratios and fractions of fatigue lives at those stress ratios. ASTM A 7 specimens were tested in completely reversed loading to failure or runout which was specified at 12 x 10^6 cycles.

Inspection after the tests were completed revealed that all fractured specimens failed at the transition between the fillet and the gage section. This did not affect the continuity of test results. There was no appreciable difference in the fatigue behavior of the eyebar and replica specimens.

None of the steels tested showed any significant loss in mechanical properties, compared to results of fatigue tests of mild steel performed by others. The two ASTM A 7 steel specimens had lower ratios of fatigue limits to ultimate strengths than values obtained by others. However, this was probably caused by the stress risers at the gage-section fillets.

Tensile AE tests were conducted on unfatigued specimens and those which had survived the specified fatigue run-out. No major differences in mechanical behavior or AE response were noted. The fatigue specimens had undergone strain aging between the time of fatigue testing and the subsequent tensile tests.

Several of these specimens were notched and tensile tested to determine the behavior of specimens with stress concentrations. Each specimen showed high strength and low ductility. AE activity of notched specimens differed from the unnotched ones. The notched specimens showed a slight increase in AE rate prior to failure.

A field test was performed using a large I-beam and an AE simulator. The simulator induced sound waves in the beam similar in frequency content and magnitude to AE waves produced by a growing crack. At high signal resolutions, the AE detection system could detect these excitations at a distance of about 45 feet (14.8 m). This shows the capability of AE testing on large structural members.

Scope

The Division of Research, Kentucky Bureau of Highways, has been concerned with the problem of bridge fatigue for the past 15 years. Most of the Division's past research used statistical models based on the analysis traffic patterns in an attempt to predict the remaining safe life of bridges *(1, 2)*. The utility of this type of analysis is limited by several facts. Bridges subject to fatigue show the cumulative effects of random cyclic loads (sometimes above the fatigue limit). Damage theories postulated by the Division of Research were based on Miner's rule, which assumes that if n_i cycles of stress σ_i are applied to a member, where N_i was the fatigue limit

for the member, failure could occur when

$$(\Sigma\ n_i/N_i) = 1.$$

Miner's rule has not proven conservative and is subject to the same statistical variations encountered in fatigue tests. Also, in its simplest form, it precludes the possibility of a pre-existent crack which can easily occur in a structure as large as a bridge.

It was realized that some information on actual material performance would be required to substantiate assumptions incorporated in earlier statistical models. Little previous research could be found on the mechanical performance of steels subjected to many years service in a fatigue environment. Acoustic emission, a new laboratory and nondestructive evaluation tool, showed some potential for providing data about the loading history of a material. Therefore, a study was initiated to investigate acoustic emission and fatigue.

Acoustic Emission

Acoustic emissions (AE) are transient, elastic waves generated by the rapid release of energy from a material subjected to an external stress. Consider breaking a stick by slowly bending it: when the wood fibers fracture, a noise can be heard. However, most dynamic processes in metal release insufficient energy to be detected audibly. Therefore, sensitive electronic equipment is required to detect these processes.

A schematic diagram of the Dunegan Model 3000 acoustic emission detector used in the study is shown in Figure 1. The essential components are transducers, preamplifiers, and totalizers (counters). Transducers receive weak, high-frequency mechanical vibrations from dynamically stressed specimens and converts them into electrical signals proportional to the rate and the intensity of the impressed vibrations. Preamplifiers amplify the signals, filtering out frequencies below 100 kHz, which are usually extraneous mechanical noises. The totalizers (counting circuitry) measure and count the voltage signals from the preamplifier that exceed a certain threshold level. This data is displayed as 'counts', being proportional to the frequency and intensity of the impressed vibrations. The totalizer can work in conjunction with a Dunegan Model 402 reset clock to provide count rates. Counting is visually displayed on a panel meter and on a strip chart. The amplified signal is heard through a Dunegan Model 702 audio monitor. The couplant used in this study to connect transducers to test specimens was a viscous polyester resin, Dow DV-9.

Initial Acoustic Emission Tests

Several basic questions needed to be answered about the exact physical sources of acoustic emission before any correlation could be made between acoustic emission and fatigue. Ingham, et al., associated the AE phenomena in steel with cracking of cementite *(3)*. They noted that steels with spheriodized peralite produce less total acoustic emission than those with lamellar pearlite. Dunegan and Harris, however, associated AE activity with mobile dislocations *(4)*.

Figure 1. Acoustic Emission Detection System.

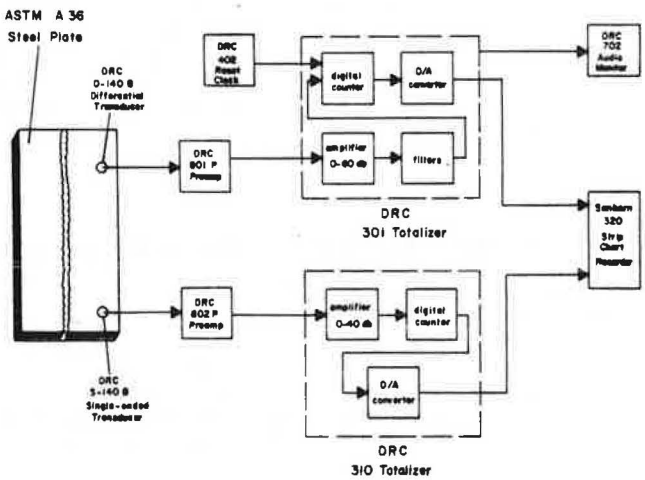

A series of tensile and compressive tests was performed on steel and aluminum specimens. The tests were conducted at the University of Kentucky Department of Metallurgical Engineering and Materials Science using a 20,000-pound (88,960-N) capacity, universal testing machine (Instron). Pin-type grips were required for tensile specimens. A special prestressing device was used to preload pin holes. The preload was higher than fracture load of the specimens. This had two beneficial effects: it work-hardened the specimen pin holes, and it 'silenced' noise from deformation at the pin holes. This minimized AE activity from the grip area during the tests.

The initial tensile tests, shown in Figure 2, were conducted using AISI 1018 steel specimens. The resulting load- and AE rate-versus-strain curve of Figure 3 shows a difference between cold-worked AISI 1018 steel (Test 9) and annealed AISI 1018 steel (Test 10). These tests were run at a crosshead speed of 0.05 in./min (1.3 mm/min). Low-noise (differential) Dunegan D140 transducers were used for the tests. Acoustic emissions were summed over a time interval of two seconds to give a rate indication of AE activity. The Model 301 totalizer was run with a gain of 95 dB. The AE output of the totalizer was plotted on a strip-chart recorder.

Figure 2. Tensile/AE Test of a Steel Specimen.

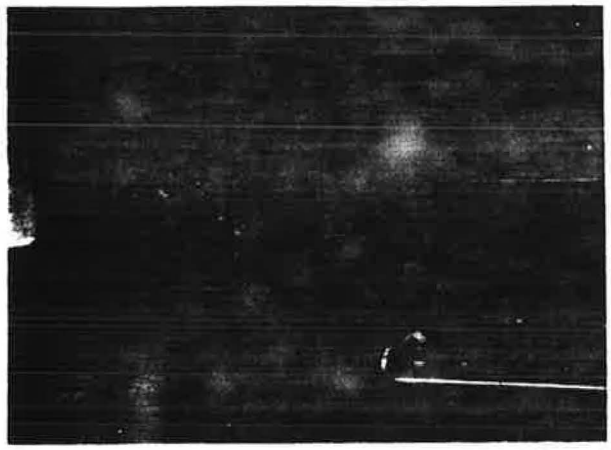

AE activity of cold-worked steel increased rapidly with the rising tensile load and reached a maximum value at the proportional limit. After plastic deformation began, the AE activity decreased. The AE rate for the annealed specimen increased gradually with load, reaching a maximum value at the proportional limit. After plastic deformation began and as it proceeded, the AE rate decreased. Whereas the cold-worked steel had the highest AE rate, the annealed steel had nearly three times as many total AE counts. Most of the potential for AE activity in the cold-worked steel had been dissipated by creating dislocations in the cold-forming process; therefore, less total AE activity was possible.

Figure 4 demonstrates the irreversibility of acoustic emissions with loading, using the fully annealed steel. The summing interval was increased to 10 seconds. The specimen was loaded until discontinuous yielding took place. Then, the load was decreased to a low value. The specimen was reloaded and pulled to failure. The AE rate curve demonstrated the irreversibility of acoustic emission. AE activity ceased on unloading, and no emissions occurred until the previous maximum load was exceeded. This behavior, called the Kaiser effect, was found to exist for both elastic and plastic deformation.

Figure 5 shows the load- and AE rate-vesus-strain for a one-inch (25.4-mm) cube of commercially pure aluminum in compression. The Kaiser effect was also demonstrated in this test. The specimen was strained at a crosshead rate of 0.01 in./minute (0.254 mm/minute). A 2-second summing interval was used for the AE rate. No AE activity was found until the proportional limit was exceeded. The maximum AE rate occurred prior to the onset of gross plastic flow. The AE activity, for most aluminum specimens tested, decreased gradually with increasing plastic flow. The compression test was stopped when the load reached the maximum capacity of the testing machine.

The ductile aluminum specimen shown in Figure 5 had approximately the same volume of material subject to maximum strains as the steel specimens. The rate of AE activity from the aluminum specimen is of the same order of magnitude as the AE rate from the steel specimens. Commercially pure aluminum has no brittle second phase such as cementite.

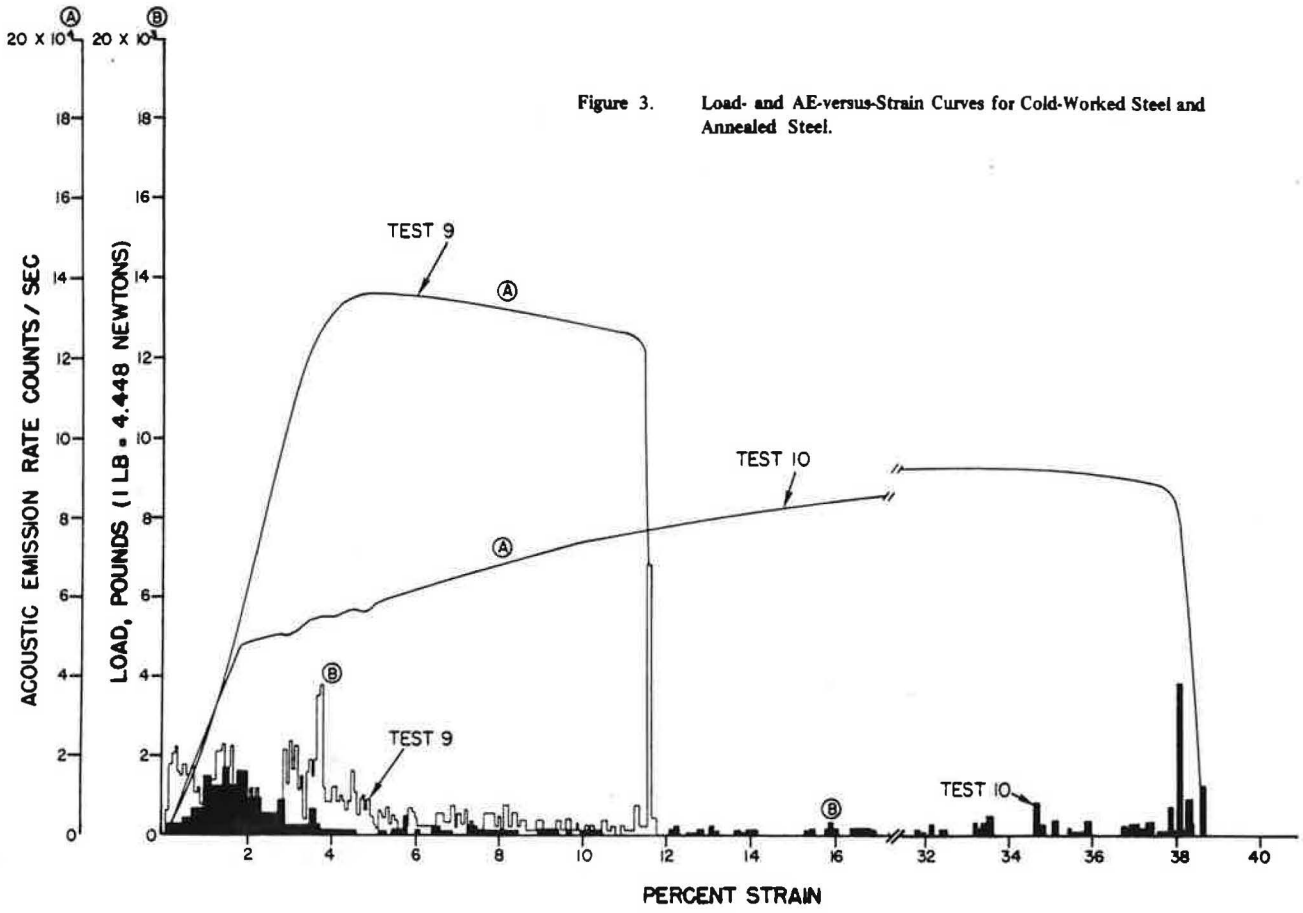

Figure 3. Load- and AE-versus-Strain Curves for Cold-Worked Steel and Annealed Steel.

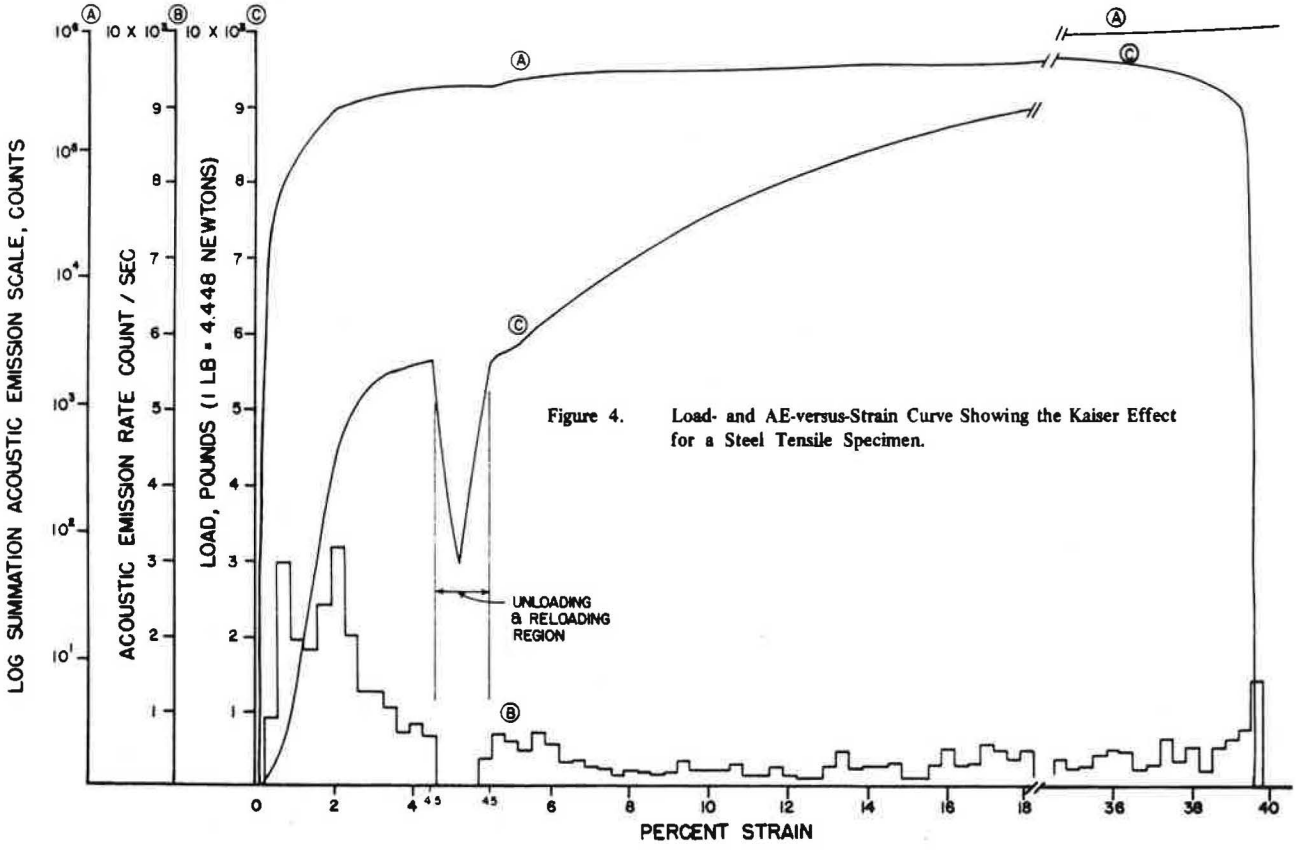

Figure 4. Load- and AE-versus-Strain Curve Showing the Kaiser Effect for a Steel Tensile Specimen.

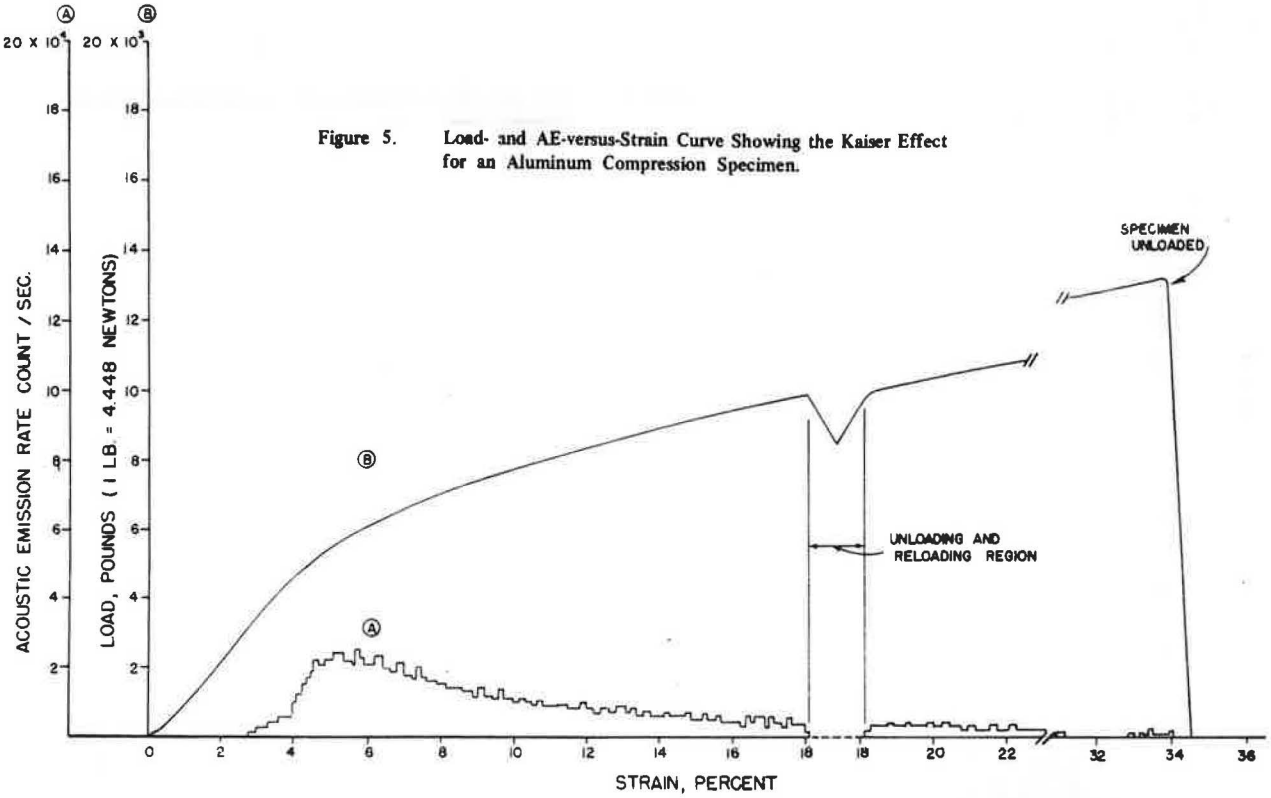

Figure 5. **Load- and AE-versus-Strain Curve Showing the Kaiser Effect for an Aluminum Compression Specimen.**

The source of AE activity in this metal must be attributed to dislocation motion *(5, 6, 7)*. The decrease of mobile dislocations, with the continuation of plastic flow and work-hardening, closely correlates with the AE-rate behavior of aluminum due to the greater ease of dislocation motion in the face-centered cubic metal. A ductile phase of steel, ferrite, must also be capable of producing a significant amount of acoustic emission. The contribution of cementite fracture to the total AE activity in a structural steel must be dependent on the percentage present. In most structural steels, the cementite content is very small.

The difference between AE rates of the cold-worked and annealed AISI 1018 steels is better explained by dislocation motion. The initial dislocation density of the cold-worked steel was from 10^2 to 10^4 times greater than the annealed steel. Immediately on load application, many dislocations became mobile. Dislocations were created in the annealed steel upon loading. Therefore, the annealed steel showed a more gradual increase in AE rate and a greater total amount of AE activity.

Tests at different crosshead speeds showed that AE activity would increase with increased loading rates. AE activity was perceptable at crosshead rates as low as 0.001 in./minute (0.025 mm/minute). The Kaiser effect persisted at crosshead speeds as high as 0.7 in./minute (17.8 mm/minute). Steel specimens cut in the transverse rolling direction and normal specimens cut in the longitudinal rolling direction were tested and compared. Both types of specimens exhibited the same yield and ultimate strengths. However, the transverse-cut specimens showed 5-percent less elongation and about 80-percent less total acoustic emission.

Tensile specimens were cut from an 80-year old bridge eyebar, from the C&O bridge at Covington, which had lain in a storage yard for a year since the bridge was demolished. Specimens were cut from the eyebar stem parallel to the loading direction. It was hoped that the Kaiser effect would give an indication of the maximum service stress. However, tests revealed behavior similar to that of AISI 1018 steel. Strain aging had probably erased the Kaiser effect.

Fatigue Testing

A series of axial-fatigue tests were planned, using four types of steel. Steel from the C & O bridge eyebar was duplicated by National Steel Corporation (see Table 1). The old bridge specification was typical for acid-Bessemer steel. To duplicate the eyebar steel, National Steel Corporation phosphorized an open-hearth steel plate after it was rolled. A 7-in. x 4-in. x 1/2-in. (178-mm x 102-mm x 13-mm) unequal angle and a C9x15 channel member were also incorporated in these tests. Both were from riveted members, about 40 years old, and were presumed to be ASTM A 7. Both of these beams failed by fatigue in bridge service. The tensile strength of the angle specimen was 54.9 ksi (378 MPa), and the tensile strength of the channel specimen was 55.1 ksi (380 MPa). A typical specimen is shown in Figure 6. The specimens were cut in the logitudinal rolling direction of the steels. All natural surfaces were preserved, and all machined surfaces were ground.

The 11 C&O (Series A) specimens and the National Steel (Series B) specimens were fatigued at various stress ratios and fractions of fatigue lives at those stress ratios. Angle (Series C) and channel (Series D) specimens were tested in completely reversed loading to determine their endurance limits. The fatigue tests were run by Metcut Research Associates of Cincinnati, Ohio, on a Baldwin-Lima-Hamilton, IV-20 fatigue machine. Loading alignment was achieved by drilling pin holes, centered along the gage length of a specimen. The specimens were tested in air at room temperatures (70 ± 10 F (21 ± 5.5 C)). The specimen temperature was limited to 200 F (93 C). Loading was applied in a sinusoidal manner at the rate of 1200 cpm. The total dynamic load error was limited to ± 3 percent of the applied stress.

Test results are shown in Table 1. The fatigue limit (also the runout) was 12 x 10^6 cycles. On inspection of the specimens, after machining, some discontinuity was found between the fillet radii and the ground faces of the gage sections. This was not corrected as it was feared that any subsequent grinding would undercut the specimens at the gage root. All failed specimens fractured at this location. However, the continuity of the results suggests that the stress concentration factors which contributed to the failures were almost constant for all specimens. Plastic flow in specimens stressed greater than 30 ksi (207 MPa) led to buckling and caused three Series D tests to be aborted.

Figures 7 and 8 show modified Goodman diagrams for the Series A and B fatigue tests *(8)*. The average lines indicate average fatigue limits of new low-carbon structural steel for fatigue lives of 100,000 and 200,000 cycles. The shaded areas show stress variations between the average and minimum fatigue limits. Imposed on Figure 7 are the points representing test failures which occurred at fatigue lives greater than two million cycles. Figure 8 shows points representing test failures which occurred at fatigue lives between 96,000 and two million cycles. Figure 7 reveals that even though most of these fatigue tests lasted six times longer than values for fatigue lives of two million cycles, their fatigue limits usually equalled or exceeded the established minimum fatigue limits of typical steels for two million cycles. Figure 8 shows that fatigue limits of most specimens having

Table 1. Results of Axial Fatigue Tests

SPECIMEN NUMBER	MAXIMUM STRESS (KSI)	MINIMUM STRESS (KSI)	CYCLE DESIGNATION	CYCLE REQUIRED	CYCLES TO FAILURE (THOUSANDS)	RESULTS
A1	19	-19	NA1	TO FAILURE	12,000	FAILURE
A2	29	-29	NA2	75% OF NA5	86	FAILURE
A3	29	-29	NA3	50% OF NA5	600	REMOVED
A4	29	-29	NA4	TO FAILURE	611	FAILURE
A5	29	-29	NA5	TO FAILURE	1,197	FAILURE
A6	35	0	NA6	TO FAILURE	204	FAILURE
A7	35	0	NA7	75% OF NA6	153	REMOVED
A8	35	0	NA8	50% OF NA6	102	REMOVED
A9	54	0	NA9	TO FAILURE	96	FAILURE
A10	50	25	NA10	TO FAILURE	12,154	RUNOUT
A11	56	28	NA11	TO FAILURE	526	FAILURE
B1	29	-29	NB1	TO FAILURE	181	FAILURE
B2	29	-29	NB2	75% OF NB1	136	REMOVED
B3	35	0	NB3	TO FAILURE	12,057	RUNOUT
B4	35	0	NB4	75% OF NB3	3,985	FAILURE
B5	35	0	NB5	50% OF NB3	6,000	REMOVED
C1	25	-25	NC1	TO FAILURE	108	FAILURE
C2	25	-25	NC2	TO FAILURE	48	FAILURE
C3	30	-30	NC3	TO FAILURE	19	FAILURE
C4	30	-30	NC4	TO FAILURE	20	FAILURE
C5	20	-20	NC5	TO FAILURE	672	FAILURE
C6	20	-20	NC6	TO FAILURE	1,627	FAILURE
C7	10	-10	NC7	TO FAILURE	12,000	RUNOUT
C8	15	-15	NC8	TO FAILURE	12,143	RUNOUT
C9	19	-19	NC9	TO FAILURE	1,550	FAILURE
C10	18	-18	NC10	TO FAILURE	1,762	FAILURE
C11	16	-16	NC11	TO FAILURE	6,998	FAILURE
C12	16	-16	NC12	TO FAILURE	4,712	FAILURE
D1	45	-45	ND1	TO FAILURE		TEST ABORTED
D2	40	-40	ND2	TO FAILURE		TEST ABORTED
D3	30	-30	ND3	TO FAILURE	64	FAILURE
D4	30	-30	ND4	TO FAILURE	99	FAILURE
D5	20	-20	ND5	TO FAILURE	835	FAILURE
D6	20	-20	ND6	TO FAILURE	1,169	FAILURE
D7	10	-10	ND7	TO FAILURE	15,395	RUNOUT
D8	19	-19	ND8	TO FAILURE	1,832	FAILURE
D9	15	-15	ND9	TO FAILURE	12,000	RUNOUT
D10	18	-18	ND10	TO FAILURE	12,000	RUNOUT
D11	19	-19	ND11	TO FAILURE	474	FAILURE
D12	35	-35	ND12	TO FAILURE		TEST ABORTED

NOTES: POSITIVE STRESS DENOTES TENSION
NEGATIVE STRESS DENOTES COMPRESSION
1 KSI = 6.895 MPa

fatigue lives of approximately 100,000 cycles met or exceeded the minimum fatigue limits of typical structural steels. Most specimens with fatigue lives approaching two million cycles had slightly lower fatigue limits than the average values given for typical steels with 100,000-cycle lives. However, these specimens had higher fatigues limits than typical steels with fatigue lives of two million cycles. The Series C and Series D specimens both had fatigue limits of approximately 15 ksi (103 MPa).

The yield and ultimate strengths of the National Steel (Series B) specimens were greater than those of the C&O eyebar (Series A) specimens. Therefore, higher fatigue limits were expected from the National Steel specimens. The maximum ratios of the fatigue limit to the ultimate strengths for the angle and channel specimens were 0.27 and 0.26, respectively. These values are in the lower range of this ratio as compiled by others *(8)*. The low values are attributable to stress risers at the gage-section fillets.

Thirty days after the fatigue tests ended, tensile/AE tests were performed on some untested specimens and specimens which survived the fatigue tests. Prior to each test, the coupling efficiency between a specimen and a transducer was measured using a Trodyne, 'Sim-Cal', spark-gap, AE calibration device. The 'Sim-Cal' duplicates an AE wave source with a signal repeatable within ± 20 percent. The average number of AE counts recorded by the AE detector from ten 'Sim-Cal' excitations was used in a simple ratio between the lowest average (as a reference) and the average of other tests to standardize data. The specimen pin holes were preloaded, and the tests were performed at a crosshead speed of 0.05 in./minute (1.3 mm/minute). The gain was set at 95 dB with high-pass filtration of 0.1 MHz. Thirteen specimens were tested to failure. Three were loaded to their yield points, removed, notched, and tested to failure. The results of these tests are shown in Table 2.

The tests revealed that the specimens had strain aged. The AE rate curves resembled those of earlier tests, and the Kaiser effect was not evident. There was no discernible effect on the mechanical properties of the specimens subjected to low-level cyclic stresses. A C&O eyebar specimen (A 11), fatigued in the range from 56 ksi (386 MPa) to 28 ksi (193 MPa) for 12 million cycles, differed little in ductility and toughness from specimens which had not been fatigued.

It became apparent that no gross changes in mechanical behavior resulted from cyclic loading below the yield region. One C&O eyebar specimen (A3) produced an unusually high AE count. Most of the activity

Figure 6. National Steel (Series B) and Angle (Series D) Fatigue Specimens.

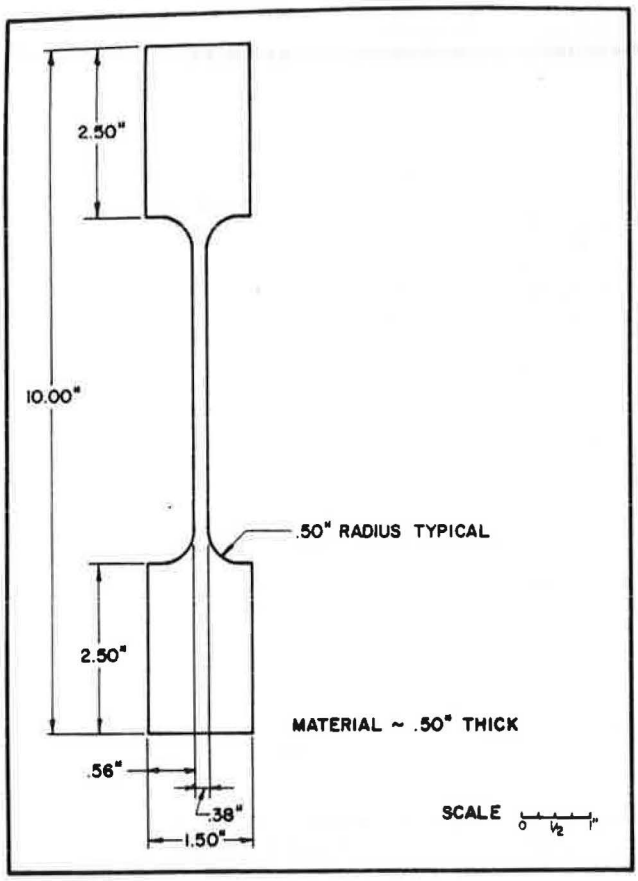

Figure 7. Modified Goodman Diagrms Comparing Fatigue Limits of Bridge Steels with Average Values, for Fatigue Lives Greater than 2,000,000 Cycles *(14)*.

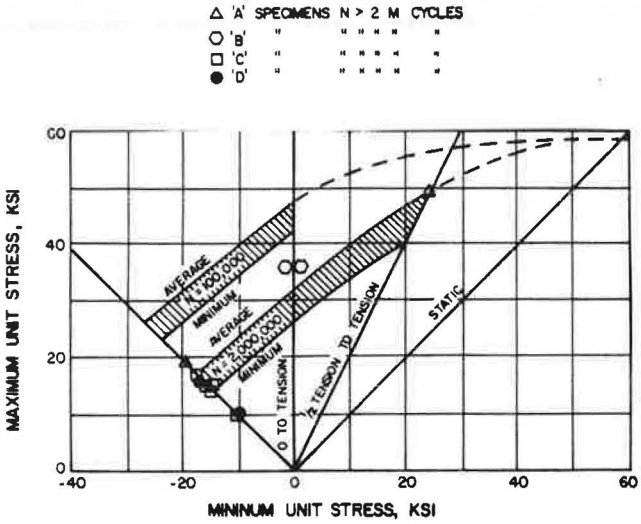

Figure 8. Modified Goodman Diagram Comparing Fatigue Limits for Bridge Steel with Average Values, for Fatigue Lives Less than 2,000,000 Cycles and Greater than 96,000 Cycles.

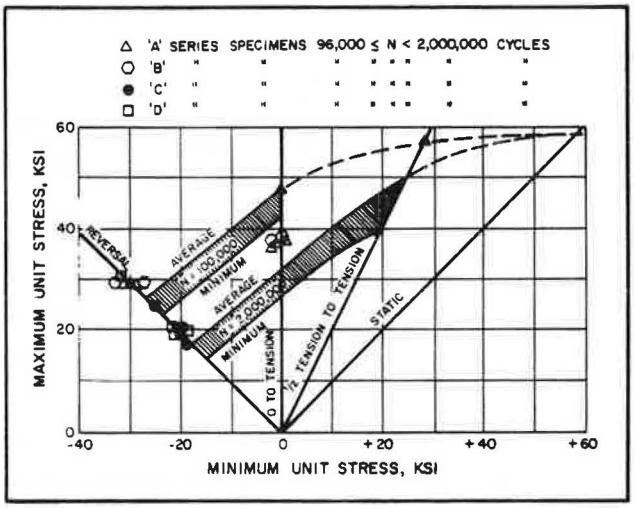

Table 2. Tensile Test Data for Fatigue-Tested Specimens

SPECIMEN NUMBER	FATIGUE LOAD (KSI)	NUMBER OF CYCLES (THOUSANDS)	REDUCTION IN AREA (PERCENT)	ELONGATION (PERCENT)	ULTIMATE STRESS (KSI)	2% YIELD STRESS (KSI)	VOLUME IN TEST ($IN.^3$)	TRODYNE COUNTS (AVERAGE)	TOTAL CORRECTED ACOUSTIC EMISSION COUNTS	TOUGHNESS ($IN.-KIP/IN.^3$)
A1	19 TO -19	12,000	61.4	24.6	55.85	35.10	0.7973	13.5	331.5	30.38
A3	29 TO -29	600	58.4	22.6	57.80	36.99	0.7268	12.6	1,039.6	31.75
A7*	35 TO 0	153	23.0	12.0	64.94	47.58	0.7875	9.5	2,455.6	14.13
A8	35 TO 0	102	60.7	22.0	56.83	36.08	0.7165	9.4	417.3	30.63
A11	56 TO 28	12,150	59.4	21.0	62.15	53.55	0.8019	11.6	290.6	28.88
A12*			62.4	23.0	57.13	36.35	0.6179	15.5	536.0	28.13
B2	29 TO -29	136	57.4	29.3	62.96	38.60	0.8025	7.7	230.4	40.25
B3	35 TO 0	12,050	57.6	27.7	62.43	37.83	0.8014	7.1	78.7	39.38
B5	35 TO 0	6,000	57.3	31.6	64.17	38.77	0.7835	6.2	240.5	42.25
B6*			58.9	31.4	61.37	36.46	0.8118	10.3	191.3	42.38
C7	10 TO -10	12,000	54.2	41.2	62.24	36.36	0.4776	6.6	60.9	58.13
C8	15 TO -15	12,140	50.2	8.1	71.78	52.38	0.4491	5.9	1,913.4	8.50
D6	15 TO -15	12,000	60.4	29.7	57.57	38.90	0.8059	14.0	382.9	37.00
D7	10 TO -10	15,400	80.2	27.2	58.47	40.68	0.8099	16.0	55.5	35.75
D10*	18 TO -18	12,000	22.8	10.8	68.69	52.84	0.7846	11.3	322.5	12.38
D12**	35 TO -35	TEST STOPPED	59.2	21.5	58.69	38.95	0.8047	14.5	57.5	27.38

NOTES: * NOTCHED
** DAMAGED
1 KSI = 6.895 MPa
1 IN. = 163.9 mM
1 $IN.-KIP/IN.^3$ = 2.756 MJ/M^3

occurred in the discontinuous yield region. However, the mechanical properties measured during this test did not markedly differ from values of other specimens. This event represents some presently undetermined variance in properties not measurable by tensile testing.

Three specimens (A7, C8, and D10) were notched with a jeweler's hacksaw after an initial loading. After notching, the specimens were pulled to failure. During the tests, the notches were observed to become blunted, and areas of localized plastic deformation appeared on the faces of the specimens adjacent to the notches. Compared to unnotched specimens, the notched specimens showed higher yield and ultimate strengths but exhibited lower toughness and elongation. The total AE count was greater for unnotched specimens. AE activity of notched specimens began immediately with the load application. It reached a maximum value during discontinuous yielding and decreased with the onset of fully plastic flow. A slight increase in AE rate occurred prior to failure. The increase in strength and loss of ductility are results of the notch effect. The high initial rate of AE activity was caused by the rapid onset of localized plastic flow. The increase of AE rate prior to fracture was probably due to rapid growth of the plastic zone.

As a result of these tests, it became evident that no gross changes in mechanical properties had occurred in steels which had seen extended service. Also, there was no detectable difference in AE activity between any of the fatigued steels or any unfatigued steels.

Tests indicated that field fatigue failures should be viewed as discrete events which were much more difficult to characterize than laboratory-derived values such as the yield strength or even the fatigue limit. This led to the view that material properties were not of prime importance, especially when compared to geometric factors (stress risers).

Field Testing

AE systems have been interfaced with computers to locate defects in pressure vessels for the past 12 years. Much field experience has been accumulated from oil storage tanks, rocket motor cases, and nuclear reactors *(9, 10, 11)*. Several techniques have been developed for AE discrimination in a high noise environment *(12, 13)*. However, few significant trials of AE flaw-locating equipment have been made on bridges *(14)*.

To further explore the listening and probing capabilities of equipment, a large, welded plate girder, approximately 50 feet (16.4 m) long having a web length of 27 inches (690 mm) and a thickness of 3/4 inch (19 mm) was tested using the AE device and the 'Sim-Cal' calibrator. The 'Sim-Cal' produced a repeatable, simulated acoustic pulse of lower magnitude than an AE burst in a notched tensile specimen. Using a gain of 97 dB, with band-pass filtration of 0.1 to 0.3 MHz and a single-ended Dunegan S-140B transducer, the 'Sim-Cal' signal could readily be detected from 45 feet (14.8 m) by the AE device. A decrease in AE intensity occurred with increasing distance between the transducer and the AE calibrator. However, the test showed that AE energy caused by crack blunting or growth can be detected by AE systems over long distances. Recent improvements in AE flaw-locating systems have enabled their use on geometrically complex structures and reduced the amount of electronics required to locate defects over long distances.

References

1. Havens, J. H. and Deen, R. C.; *Bridges: Synthesis of Load Histories and Analysis of Fatigue;* Division of Research, Kentucky Department of Highways, January 1972.
2. Lynch, R. L.; *Analysis of Traffic Loads on Bridges; Report II, Characteristics of Traffic on Ohio River Bridges - 1968;* Division of Research, Kentucky Department of Highways, March 1969.
3. Ingham, T., Scott, A. L. and Cowan, A.; *Acoustic Emission Characterization of Steels, Part 1: Acoustic Emission Measurements from Tensile Tests;* **International Journal of Pressure Vessels and Piping,** Applied Science Publishers, UK, February 1974, pp 31-49.
4. Dunegan, H. L. and Harris, D. O.; *Acoustic Emission - A New Nondestructive Testing Tool;* **Ultrasonics,** IPC Press, Guilford, UK, July 1969, pp 160-166.
5. Frederick, J. R. and Felback, D. K.; *Dislocation Motion as a Source for Acoustic Emission;* **Acoustic Emission,** STP 505, American Society for Testing and Materials, 1972, pp 129-139.
6. Gillis, P. P.; *Dislocation Motions and Acoustic Emissions;* **Acoustic Emission,** STP 505, American Society for Testing and Materials, 1972, pp 20-29.
7. James, D. R. and Carpenter, S. H.; *Relationship between Acoustic Emission and Dislocation Kinetics in Crystalline Solids;* **Journal of Applied Science,** AIP, Menasha, Wis, November 1971, pp 4685-4697.
8. Munse, W. H.; *Fatigue of Welded Steel Structures;* Welding Research Council, 1964, p 36, 37, 74.
9. Tatro, C. A.; *Design Criteria for Acoustic Emission Experimentation;* **Acoustic Emission,** STP 505, American Society for Testing and Materials, 1972, pp 84-99.
10. Cross, N. O., Loushin, L. L., and Thompson, J. L.; *Acoustic Emission Testing of Pressure Vessels for Petroleum Refineries and Chemical Plants;* **Acoustic Emission,** STP 505, American Society for Testing and Materials, 1972; pp 270-296.
11. Harris, D. O. and Dunegan, H. L.; *Acoustic Emission 5 - Application of Acoustic Emission to Industrial Problems;* **Nondestructive Testing,** IPC Press, Guilford, UK, June 1974, pp 137-144.
12. Liptai, R. G., Harris, D. O., Engle, R. B., and Taro, C. A.; *Acoustic Emission Techniques in Materials Research;* **International Journal of Nondestructive Testing,** May 1971, pp 215-175.
13. Nakamura, Y.; *Acoustic Emission Monitoring System for Detection of Cracks in Complex Structures;* **Materials Evaluation,** ASNT, Columbus, OH, January 1971, pp 8-12.
14. Pollock, A. A. and Smith, B.; *Stress Wave-Emission Monitoring of a Military Bridge;* **Nondestructive Testing,** IPC Press, Guilford, UK, December 1972, pp 348-353.